Molecular basis for the explanation of the exponential growth of polyelectrolyte multilayers

C. Picart*†, J. Mutterer‡, L. Richert*, Y. Luo§, G. D. Prestwich§, P. Schaaf†¶‖, J.-C. Voegel*, and P. Lavalle*

*Institut National de la Santé et de la Recherche Médicale, Unité 424, Centre de Recherche Odontologique, Université Louis Pasteur, 11 Rue Humann, 67085 Strasbourg Cedex, France; †Ecole Européenne de Chimie, Polymères et Matériaux de Strasbourg, 25 Rue Becquerel, 67087 Strasbourg Cedex 2, France; ‡Institut de Biologie Moléculaire des Plantes, 12 Rue du Général Zimmer, 67084 Strasbourg Cedex, France; §Department of Medical Chemistry, University of Utah, Salt Lake City, UT 84112-5820; and ¶Institut Charles Sadron (Centre National de la Recherche Scientifique–Université Louis Pasteur), 6 Rue Boussingault, 67083 Strasbourg Cedex, France

Communicated by Howard Reiss, University of California, Los Angeles, CA, August 12, 2002 (received for review February 4, 2002)

The structure of poly(L-lysine) (PLL)/hyaluronan (HA) polyelectrolyte multilayers formed by electrostatic self-assembly is studied by using confocal laser scanning microscopy, quartz crystal microbalance, and optical waveguide lightmode spectroscopy. These films exhibit an exponential growth regime where the thickness increases exponentially with the number of deposited layers, leading to micrometer thick films. Previously such a growth regime was suggested to result from an ''in'' and ''out'' diffusion of the PLL chains through the film during buildup, but direct evidence was lacking. The use of dye-conjugated polyelectrolytes now allows a direct three-dimensional visualization of the film construction by introducing fluorescent polyelectrolytes at different steps during the film buildup. We find that, as postulated, PLL diffuses throughout the film down into the substrate after each new PLL injection and out of the film after each PLL rinsing and further after each HA injection. As PLL reaches the outer layer of the film it interacts with the incoming HA, forming the new HA/PLL layer. The thickness of this new layer is thus proportional to the amount of PLL that diffuses out of the film during the buildup step, which explains the exponential growth regime. HA layers are also visualized but no diffusion is observed, leading to a stratified film structure. We believe that such a diffusion-based buildup mechanism explains most of the exponential-like growth processes of polyelectrolyte multilayers reported in the literature.

hyaluronan | poly(L-lysine) | confocal laser scanning microscopy | diffusion | film structure

The alternating dipping of a charged surface into a polyanion and then into a polycation solution usually leads to the progressive formation of films defined as polyelectrolyte multilayers (1, 2). This electrostatic self-assembly method has been developed recently as a way for producing organic and hybrid organic-inorganic supramolecular assemblies without requiring extensive equipment. In particular, in the biomedical field, these multilayers constitute versatile tools for the design of thin films containing macromolecules such as proteins (3), nucleic acids (4), or polypeptides with targeted properties (5).

However, finding a common rule that can explain the growth mechanism for all of the systems investigated has not been straightforward. It is already known that polyelectrolyte adsorption is governed by the charge reversal that appears on the film surface after each dipping step and that constitutes the buildup motor for the assembly. Whereas some polyelectrolyte systems appear to grow linearly with the number of deposited layers, others such as poly(L-lysine) (PLL)/alginate (6), PLL/hyaluronan (HA) (7) or PLL/poly(L-glutamic acid) reveal a "exponential growth regime" (6, 8–10). This regime is characterized by the film thickness and the amount of adsorbed polyelectrolytes that increase more rapidly than linearly with the number of deposited layer pairs. Increasing the salt concentration in which the buildup takes place can lead to a transition from a linear growth regime to an exponential growth regime for the poly(styrenesulfonate) (PSS)/poly(allylamine hydrochloride) system (9) or for the polydiallyldimethytlammonium chloride/PSS (11) film architecture.

Understanding how the multilayers are structured and what governs their assembly is of great importance for tuning their physico-chemical properties. The existence of a layered structure with an interpenetration between neighboring layers was evidenced by x-ray reflectivity measurements (12) for the widely studied poly(styrenesulfonate)/poly(allylamine hydrochloride) system. Observation by transmission electron microscopy also allowed the distinction of the vertical organization of multilayer hetero-structures formed with two different polyelectrolyte systems (13). However, up to now, the resolution obtained with electron microscopy did not permit a direct visualization of a layering for a given system.

The mechanism responsible for an exponential buildup processes is not clearly understood. It was first suggested that it is due to an increase in the film roughness with the number of deposited layers. However, these films can reach thicknesses of several micrometers, which is difficult to explain by the sole influence of the film roughness. Elbert *et al.* (6) proposed that the exponential growth regime could be the consequence of a complexation process of polyanions and polycations above the film. Recent experiments on PLL/HA (14) and PLL/poly(L-glutamic acid) (PGA) (10) films suggested a diffusion of the PLL chains "in" and "out" of the film during buildup. Thus, while PLL diffuses out of the film in the presence of the polyanion (HA or PGA) in solution, PLL/polyanion complexes form at the outerlayer of the film. The thickness of the new forming layer on top of the film is then proportional to the amount of PLL chains that diffuse out of the multilayer while the polyanion is in solution, this amount being proportional to the film thickness. Such a mechanism leads to an exponential growth regime. However, while small ions are known to diffuse into polyelectrolyte multilayer films, the diffusion of polyelectrolytes into multilayer films was never observed. The only indirect evidence of such a diffusion process over the entire film is provided by changes in optical signals when a film, whose thickness was expected to be of the order of 1 μm, was brought in contact with a PLL solution, the optical method being only sensitive to the part of the film that covers the penetration zone (of the order of 200 nm) of an evanescent wave (7).

In the present work we first demonstrate the existence of such a polyelectrolyte diffusion process into polyelectrolyte multilayer films that exhibit an exponential growth regime. Taking advantage of the fact that one can reach micrometer thick films for these systems we use confocal microscopy to visualize *in situ* the location of the polyelectrolytes constituting the films. Second, we also follow directly the film buildup process and observe an eventual layering despite diffusion. The visualization of the in

Abbreviations: HA, hyaluronan; PLL, poly(L-lysine); CLSM, confocal laser scanning microscopy; OWLS, optical waveguide lightmode spectroscopy; TR, Texas red; QCM, quartz crystal microbalance.

‖To whom reprint requests should be addressed. E-mail: schaaf@ics.u-strasbg.fr.

and out diffusion process of one of the polyelectrolytes represents a direct validation of the postulated buildup mechanism responsible for the exponential growth regime. The fact that a system grows "linearly" or "exponentially" should thus be related to the ability of at least one of the polyelectrolytes to diffuse in and out of the films.

We use the PLL/HA system, a polyelectrolyte pair selected for their exponential growth regime (14). Both HA and PLL are widely used in biomedical engineering. HA is a polysaccharide glycosaminoglycan present in the extracellular matrix, the synovial fluid, and the eye aqueous humor (15, 16) with the ability to form viscoelastic aqueous solutions in consequence of the entanglement interactions between domains (17). PLL was chosen not only because it is biocompatible (18), but also because it offers the possibility of being easily conjugated with bioactive molecules (19). The films containing PLL/HA are expected to be highly hydrated because both polyelectrolytes are hydrophilic. For PLL, the amount of water uptaken can be as high as 50% (wt/wt) (20) and HA hydrates by taking up as much as 1,000-fold its dry weight (21). Therefore, for such systems, it is crucial to study the film structure *in situ* to avoid artifacts introduced by drying, extensive fixation, or embedding protocols.

Materials and Methods

Polyelectrolytes and Solution. HA (as sodium hyaluronate, 2.3×10^5 Da) was a generous gift from Bioiberica, Barcelona (J. Gomez). HA is a polyanionic macromolecule (1 carboxylic acid/disaccharide unit) with a pKa $\approx$2.9 (15) and hence a net charge of -1 at physiological pH. SDS and PLL (3.03×10^4 Da) were purchased from Sigma. PLL is a positively charged polyelectrolyte in physiological conditions with a pKa $\approx$9 (22). Sodium chloride (purity 99.5%) was obtained from Fluka. All solutions were prepared by using Ultrapure water (Milli Q-plus system, Millipore) with a resistivity of 18.2 MΩ·cm.

The experiments were performed by using polyelectrolyte solutions prepared by direct dissolution at 1 mg/ml (or 20 mg/ml when explicitly mentioned in the text) of HA and PLL in 0.15 M NaCl in water and were gently stirred for several hours. The pHs of the water and the PLL and HA solutions were in the range of 6 to 6.5.

Fluorescently Labeled Polyelectrolytes. PLL labeled with FITC (5.02×10^4 Da) was purchased from Sigma. The degree of substitution is of 7 mmol FITC per lysine monomer, and the degree of polymerization determined by low angle laser light scattering is 461.

HA labeled with Texas red (TR) was prepared as described with modifications. HA (1.5×10^6 Da, Clear Solutions Biotech, Stony Brook, NY) was subjected to acid degradation to give 2×10^5 Da as determined by gel permeation analysis. Reaction of HA with adipic dihydrazide (ADH, Aldrich; refs. 23–26) was modified as published to give a high-purity HA-ADH product with 20% of the carboxylic acid groups modified as determined by proton NMR (25). Next, a stirred, 4°C solution of 100 mg of HA-ADH was dissolved in 20 ml H_2O and treated with a solution of 1.3 mg TR succinimidyl ester (30 mmol; Molecular Probes) in 10 ml dimethylformamide. The reaction mixture was purified on a Sephadex G-25. The homogeneity of the HA-TR was determined by gel permeation analysis and monitored at 593 nm (TR) and 210 nm (HA absorption). The aqueous eluate was lyophilized, and the degree of substitution of the HA-TR was determined to be 0.015 fluorophores per HA disaccharide.

Confocal Laser Scanning Microscopy (CLSM). For CLSM, the multilayers were deposited on borosilicate glass slides (LabTek chambers, Nalge Nunc), preliminarily cleaned with 10 mM SDS and 0.1 M HCl and extensively rinsed. PLL was first adsorbed by deposition of 200 μl in a well and left at rest for 12 min. PLL solution was removed and two rinsing steps were performed by deposition of 200 μl of 0.15 M NaCl solution at each time. HA was then deposited and subsequently rinsed following the same procedure. All of these deposition and rinsing steps were performed with a micropipette. The dye-conjugated polyelectrolytes, HA-TR and PLL-FITC, were adsorbed in the same way at a certain stage of the buildup. As an example, $(PLL/HA)_{19}$–PLL_{20}-FITC means that the film is composed of 19 pairs of layers deposited in 19 cycles, on the top of which a final layer of PLL_{20}-FITC has been adsorbed. Each film observed at a given stage of the construction corresponds to a totally new buildup.

CLSM observations were carried out on a Zeiss LSM 510 microscope. FITC fluorescence was detected after excitation at 488 nm, cutoff dichroic mirror 488 nm, and emission band pass filter 505–530 nm (green). TR fluorescence was detected after excitation at 543 nm, dichroic mirror 543 nm, and emission long pass filter 585 nm (red). All observations were done by using a $\times 63/1.4$ oil immersion objective with pinhole sizes yielding 0.7 and 0.9 μm thick z-sections in the respective channels. To image the entire film, consecutive z-sections were collected at 0.4-μm intervals. Vertical sections were created and allowed determination of the thickness of the film.

Quartz Crystal Microbalance (QCM). The measurements were performed by using the QCM system from Q-Sense (Götenborg, Sweden). QCM consists of measuring the changes in the resonance frequency Δf of a quartz crystal (27, 28), when material is brought from solution (29). The crystal is excited at its fundamental frequency (about 5 MHz) and observation takes place at the third, fifth, and seventh overtones (denoted v and corresponding to 15, 25, and 35 MHz, respectively). A decrease in $\Delta f/v$ is usually associated, in a first approximation, to an increase of the mass coupled to the quartz. The details of the experimental setup have been presented (7), except that the crystal used for the present study was coated with a $\approx$100-nm thick SiO_2 film that is deposited by active sputter-coating. We first injected by gravity 0.5 ml of a 0.15 M NaCl solution into the measurement cell (internal volume of 100 μl). After stabilization of the signals, 0.5 ml of the PLL solution was injected by gravity, left for 10 min, and rinsed for 10 min with 0.15 M NaCl solution. During these time periods, the shifts in Δf were continuously recorded. The same procedure was then used for the deposition of HA by introducing 0.5 ml of the HA solution. The buildup process was continued by the alternated PLL and HA addition up to the 12th pair of layers.

Optical Waveguide Lightmode Spectroscopy (OWLS). The $(PLL/HA)_n$ film buildup process (n being the number of deposition cycles or layer pairs) was followed by OWLS. Briefly, OWLS is an optical technique in which an evanescent wave is sensing the film. It is thus sensitive to the film structure over a distance of the order of the penetration depth of the evanescent wave near the waveguide surface (roughly over 200 nm). It gives access to the optical properties of the film (30, 31). Details of the experimental setup (7) and the analysis of the optical data (14) can be found elsewhere. At the beginning of the experiment, 0.15 M NaCl solution was flushed through the measurement cell (internal volume of 37 μl) at a constant flow rate (10 ml/h) with a syringe-pusher until constant values of the incoupling angles were reached. Then, the buffer flow was stopped and 100 μl of the PLL solution was manually injected in the cell. When a stable adsorption signal was obtained, the buffer flow was restarted for about 15 min to rinse the excess material from the cell. In the same way we continued with the alternate adsorption of HA and PLL on the waveguide.

Results and Discussion

CLSM. In a previous study (7), the PLL/HA multilayer film buildup was followed by atomic force microscopy imaging. It was

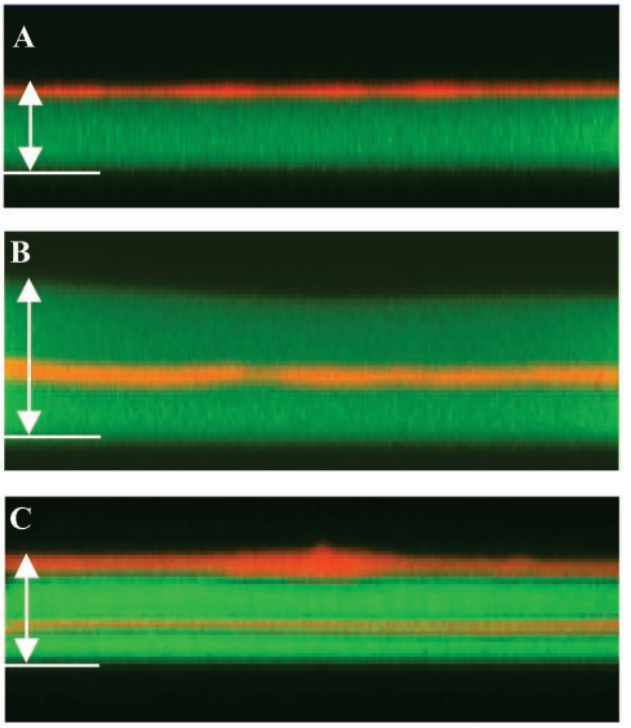

Fig. 1. Vertical sections through different film architectures containing labeled polyelectrolytes (HA-TR, red; PLL-FITC, green) obtained from CLSM observations. The borosilicate substrate (bottom of the chamber) is indicated with a white line. (*A*) $(PLL/HA)_{19}$-PLL_{20} multilayer containing two labeled layers, PLL_{19}-FITC and HA_{19}-TR. The image size is 26.2 μm $\times$ 8.4 μm. Green fluorescence (corresponding to PLL-FITC) is visible over a total thickness of around 4 μm (white arrow). (*B*) $(PLL/HA)_{25}$ multilayer containing two labeled layers, PLL_{19}-FITC and HA_{19}-TR. The image size is 36.6 μm $\times$ 14.4 μm. Green fluorescence is visible over a total thickness of around 8.0 μm (white arrow). (*C*) $(PLL/HA)_{20}$ multilayer in which the 14th and 20th HA layers are labeled, HA_{14}-TR and HA_{20}-TR, and in which the last PLL layer has been labeled, PLL_{20}-FITC. The image size is 36.6 μm $\times$ 18 μm. Green fluorescence is visible over a total thickness of around 5.0 μm (white arrow).

found that before the deposition of seven PLL/HA bilayers the substrate is covered by isolated islands whose size increases with n whereas after this buildup step, the film becomes continuous. Attention was thus paid only to films consisting of more than seven bilayers.

We monitored the buildup process by adding fluorescently labeled polyelectrolytes at different steps of the film construction. Fig. 1*A* represents a vertical section through a $(PLL/HA)_{19}$–PLL_{20} multilayer containing two labeled layers PLL_{19}-FITC and HA_{19}-TR. The green fluorescent zone represents a large and continuous band. This finding demonstrates that the PLL-FITC, although introduced at the outermost layer of the film, has diffused within the whole film down to the substrate. On the top of the green zone, a thinner band in which the color gradually changes from yellow to orange can be observed. There was no trace of yellow or orange anywhere else in the film. Thus, HA_{19}-TR did not diffuse within the film but remained only on its outer layer. The orange color of the outer layer indicates that it must also contain labeled PLL. By assuming that the PLL-FITC has diffused in the whole film, the thickness of the film could be estimated to be around 4 μm.

To test the hypothesis that PLL can also diffuse out of the film, a film buildup was prepared with 25 pairs of layers where PLL_{19}-FITC and HA_{19}-TR were inserted in fluorescently labeled form. Fig. 1*B* represents a typical vertical section through this $(PLL/HA)_{25}$ multilayer. A large and continuous green band was still visible whose thickness was of the order of 8 μm. The orange line corresponding to the HA-TR layer was also visible but located approximately in the middle of the green band. This finding demonstrates that PLL_{19}-FITC has diffused both in and out of the film. It also shows that HA-TR remained as a well-defined layer in the film. Finally, the thickness of the green zone extending from the orange band up to the bottom of the film was comparable or even slightly smaller than the green zone lying above this band, despite the fact that the first zone represents 19 pairs of layers and the second one only six pairs of layers. This observation supports the exponential growth behavior of these films.

We also observed a $(PLL/HA)_{20}$ multilayer in which the 14th and 20th HA (HA_{14}-TR and HA_{20}-TR) and only the last PLL (PLL_{20}-FITC) layers were labeled (see Fig. 1*C*). The vertical section through this film exhibited a large green band corresponding to the PLL that had diffused within the whole film down to the substrate and two orange bands corresponding to the HA-deposited layers. As expected for an exponential growth regime, the outer HA-TR layer was much thicker than the HA_{14}-TR layer. However, one cannot totally exclude that this effect is partially due to the fact that the outer layer of a multilayer film might be more swollen than the embedded ones. Moreover, the outer layer appeared nearly orange whereas the inner was more yellow, revealing that the HA_{14}-TR layer contained a larger amount of PLL-FITC than HA_{20}-TR. This finding indicated that the PLL that diffused out of the film when it was in contact with the HA_{20}-TR solution was constituted in a large part of unlabeled PLL.

Finally, to verify that the green color of the film is indeed due to PLL-FITC chains and not to free FITC eventually present in the PLL-FITC solution, we constructed a $(PLL/HA)_{19}$ film in which HA_{19}-TR was labeled and brought this film in contact with a FITC solution (isomer I, Sigma). The FITC concentration was equal to that of the total FITC content of the PLL-FITC solution used to deposit the PLL-FITC layer. After rinsing the film with buffer, the multilayer was imaged by CLSM. Whereas the HA-TR layer appeared in red, no green color was visible, proving that free FITC either does not penetrate into the multilayer or does not remain in the film after rinsing. The same experiment was also performed on a film ending with PLL instead of HA, and finally this has led to the same result. All of these data prove that the observed green color was indeed due to PLL-FITC chains.

QCM. Due to the large uncertainties in the determination of the film thickness by CLSM, we have followed the film buildup by QCM to be more quantitative about the exponential character of the growth regime. One observes that the frequency shift $-\Delta f$ at 5 MHz increases more rapidly than linearly with the number n of layer pairs (or bilayers), whereas at 25 and 35 MHz, $-\Delta f$ saturates for n = 11–12 (see Fig. 2). For a number of deposited bilayers larger than 12, we could no longer determine the frequency shifts. This saturation can be explained by the fact that the penetration length of the acoustic waves generated by the quartz crystal decreases when the frequency increases. One can thus expect that at 25 and 35 MHz, for n = 11 or 12, the penetration length must be of the order or smaller than the film thickness, whereas at 5 and 15 MHz, the penetration length is larger than the film thickness. In a first approximation one can thus assume that the signal at 5 MHz is sensitive to the mass of the whole film. As can be seen in Fig. 2, the evolution of the frequency shift at 5 MHz with n can be well fitted by an exponential (see *Inset*), thus strongly suggesting the exponential growth regime.

OWLS Measurements. To get information on the structural changes of the film during the in and out diffusion of PLL we also

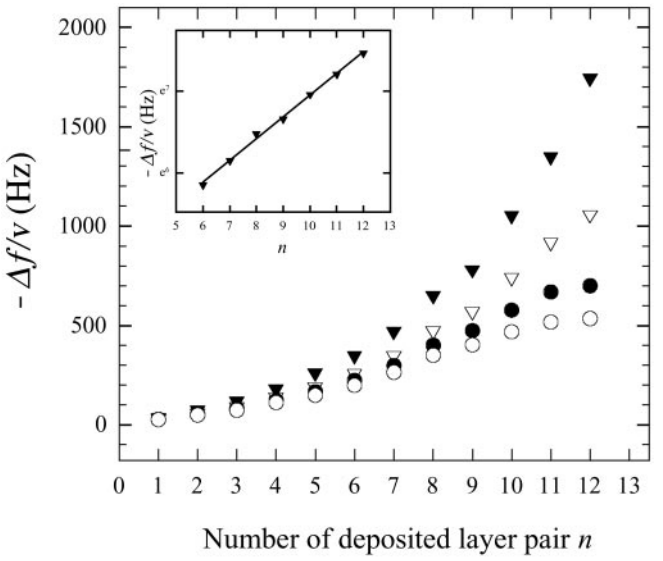

Fig. 2. Differences in the QCM frequency shifts $-\Delta f/v$ as a function of the number of layer pair n deposited on SiO_2 substrate. Data are given for four harmonics: 5 MHz (▼); 15 MHz (▽); 25 MHz (●); and 35 MHz (○). (*Inset*) The evolution of $Y = -\Delta f/v - y_0$ as a function of n in a logarithmic scale for the fundamental frequency (5 MHz) for n = 6–12. y_0 was obtained by fitting the 5-MHz data by the function $-\Delta f/v = y_0 + a \exp(bn)$. The black line corresponds to the linear regression on this logarithmic plot. The linear dependence of l*ny* with n proves the exponential nature of the growth process.

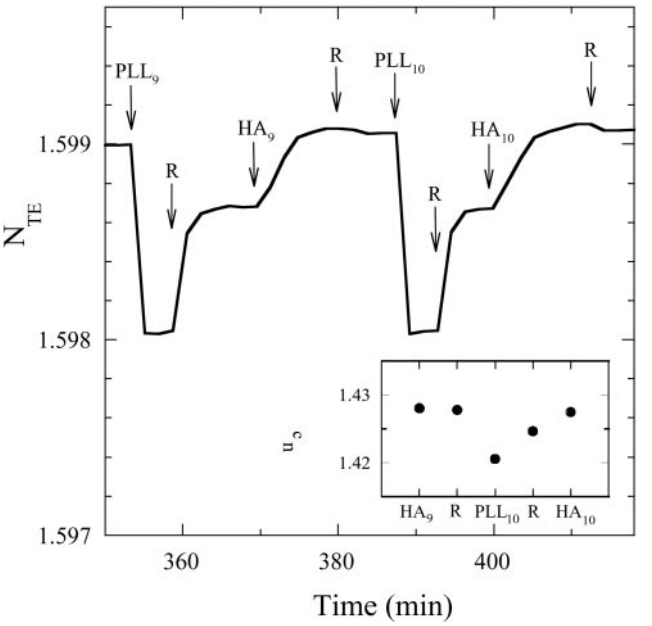

Fig. 3. Effective refractive indexes N_{TE} signal obtained by OWLS during PLL/HA multilayers buildup as a function of the time. The evolution of N_{TE} is shown over two buildup cycles once a continuous film is formed on the surface. PLL and HA were dissolved in 0.15 M NaCl at the following concentrations: PLL at 20 mg/ml and HA at 1 mg/ml. Each arrow corresponds to the beginning of the injection of either HA or PLL or only 0.15 M NaCl (corresponding in this last case to a rinsing step noted R). The number underneath PLL or HA corresponds to the layer pair deposition number. (*Inset*) The evolution of n_c, the refractive index of the film near the waveguide at the end of each buildup step during one buildup cycle.

performed OWLS experiments. This technique is only sensitive to refractive index changes in the penetration zone of the evanescent wave, which extends roughly over 200 nm. We showed in a previous study that during the initial stage of the film construction, the effective refractive indexes increase, as expected, after each new contact of the film with one of the two polyelectrolyte solutions. After several buildup cycles, the time evolution of the two effective refractive indexes changes. The refractive indexes decrease when the film is brought in contact with a PLL solution, increase during the rinsing step, increase again when the film is brought in contact with the HA solution, and remain almost constant after rinsing of the latter solution. After the deposition of some more bilayers, the evolution of the optical signals becomes perfectly cyclic from one buildup cycle to the next. This periodic behavior appears after the deposition of a smaller number of bilayers when the concentration of the PLL solution used during the film buildup is higher. It is already observed after the deposition of nine bilayers when a PLL solution of 20 mg/ml is used as can be seen in Fig. 3, where we represent a typical time evolution of the effective refractive index for transverse electric polarization N_{TE} over two buildup cycles. The same behavior is obtained for N_{TM}, the effective refractive index for transverse magnetic polarization (data not shown).

Our results do not allow us to determine the reasons only PLL and not HA diffuses within the multilayer architecture. It is known that HA molecules form a double-helical structure due to hydrophobic interactions (32). These chains can interact to form strands of HA networks composed of 15 double helixes in width and mono or double layers of the helixes in height. One may speculate that such structures render the diffusion of HA within the multilayer impossible. Other reasons such as the large persistence length of the HA chains (>10 nm) (33) and its large hydratation and strong interaction with water (34) may also contribute to hinder this diffusion.

Let us now discuss the evolution of the optical signal over one buildup cycle when the signal varies periodically (Fig. 3). When the film is brought in contact with a PLL solution (PLL_9), N_{TE} decreases over a time scale of the order of 100 s before reaching an almost constant value. Because the thickness of the film lies in the micrometer range, much larger than the penetration length of the evanescent wave, one can assume that it behaves, in first approximation, as a homogenous and isotropic infinite medium characterized by a refractive index n_c. The changes of N_{TE} and N_{TM} when the film is brought in contact with the PLL solution proves that PLL chains must diffuse down to the bottom of the film, in contact with the supporting waveguide. The refractive index of the film can be determined from N_{TE} and N_{TM} by applying the standard equations of OWLS (14). We found that the values of n_c, calculated from N_{TE} and N_{TM} were equal within 1%, proving that the homogenous and isotropic infinite medium approximation correctly describes the optical properties of this film. Within this approximation a decrease of N_{TE} and N_{TM} corresponds to a decrease of n_c. The rapid decrease of N_{TE} (and N_{TM}) thus shows that as PLL diffuses into the film, n_C decreases, which indicates that the film must swell (see Fig. 3 *Inset*). By assuming that the film thickness is of the order of 2–3 μm, one gets a diffusion coefficient of free PLL in the film of the order of 10^{-7}–10^{-8} $cm^2 \cdot s^{-1}$. This value can be compared with the value of 3×10^{-7} $cm^2 \cdot s^{-1}$ found for PLL of similar mass in solution (35). This shows that the film must be highly hydrated, as expected. One can note that the transport is not purely diffusive because a net electric field most likely exists during the film growth steps. Thus it is not surprising that this effective diffusivity is quite high. Once PLL has diffused in the film it is expected that free PLL chains can exchange other PLL chains involved in the PLL/HA complexes forming the film. Such an exchange phenomenon is generally observed when a macromolecular solution is in contact with a surface covered by adsorbed macromolecules. This exchange process explains why we observe green fluorescent chains by confocal microscopy in the upper part of the $(PLL/HA)_{25}$ multilayer even

if PLL-FITC was only used in the 19th buildup step. Once the PLL solution above the film is replaced by pure buffer, the effective refractive index N_{TE} and the refractive index n_c increase and level off at values that are smaller than their original value at the beginning of the buildup cycle. This finding indicates that free PLL diffuses out of the film during this buildup step and probably induces a deswelling of the film. However, all of the free PLL chains present in the film do not diffuse out of it. This is due to the positive charge excess that appears at the outer layer of the film once it is in contact with the PLL solution as was demonstrated by zeta potential measurements (7). This excess charge gives rise to an energy barrier located at the outer part of the film and hinders the diffusion of all of the free PLL chains out of the film. When the film is then brought in contact with the HA solution, this energy barrier disappears due to the formation of PLL/HA complexes at the outer layer. The remaining free PLL chains in the film can thus diffuse out of it. This is accompanied by a further deswelling of the multilayer leading to a further increase of n_c and thus also of N_{TE}, as observed experimentally. It is expected that, as soon as PLL chains diffusing out of the film reach the film/HA solution interface, PLL chains form complexes with HA, leading to the new HA/PLL layer. The HA solution thus acts as a perfect sink for free PLL chains in the film so that all of the free PLL chains still present in the film are strongly driven toward its outer surface. Finally, when the HA solution is replaced by pure buffer, one observes again a slight decrease of the effective refractive index. This must be due to the fact that inside the film there must always be an equilibrium between free and bound PLL chains. This equilibrium is disrupted by the presence of the HA solution that induces a deficit of free PLL chains in the film. When the HA solution is replaced by pure buffer, restructuring inside the film must take place with bound PLL chains becoming free, inducing a slight swelling of the film.

It now remains to be understood why the growth regime relative to this mechanism is exponential. After each rinsing step after the contact of the film with the PLL solution, the concentration of free PLL remaining in the film can be assumed to be the same. The amount of free PLL remaining in a film constituted of n bilayers is thus proportional to the film thickness and thus also to the amount $Q(n)$ of HA/PLL polyelectrolytes constituting the film. When this film is brought in contact with the HA solution, almost all of the free PLL chains diffuse out of the film and interact with the HA chains to form the new outer layer. The amount $\delta Q(n + 1)$ of HA/PLL polyelectrolytes constituting the new outer layer is thus proportional to the amount of free chains present previously in the film and thus to $Q(n)$. One finds that

$$\delta Q(n + 1) = K \cdot Q(n), \qquad [1]$$

where K is a proportionality constant. Finally, Eq. **1** leads to an exponential evolution of Q with the number of deposited bilayers as observed experimentally.

Conclusion

The structure of multilayer films formed by electrostatic self-assembled PLL/HA was studied by means of CLSM, OWLS, and QCM. We show that this film grows in an exponential way. It was suggested previously that such an exponential growth regime is due to the diffusion of PLL in the film. In this article, we prove the existence of such a PLL diffusion process into the interior of the film by using fluorescent-labeled PLL. Moreover, by using HA labeled with a different fluorescent probe, we also show that HA does not diffuse vertically through the film. One thus still observes a stratified film structure. We believe that most, if not all, exponential growth regimes are due to a similar in and out diffusion process of at least one of the two polyelectrolytes used in the film construction. Further experiments are now needed to be able to describe the whole buildup process more quantitatively and to predict which polyanion/polycation systems will behave in an exponential way.

We thank Prof. M. Milas (Centre d'Etudes et de Recherches sur les Macromolécules Végétalés, Grenoble, France), Prof. H. Reiss (Univ. of California, Los Angeles), and Prof. G. Decher (Institut Charles Sadron, Strasbourg) for fruitful discussions. This work was supported by the programs Action Concertée Incitative "Technologies pour la Santé" and "Surfaces, interfaces et conception de nouveaux matériaux" from the Ministère Français de la Recherche and by the Centre National de la Recherche Scientifique program "Physique et Chimie du Vivant." P.L. is indebted to the Institut Français pour la Recherche Odontologique for financial support. The CLSM platform used in this study was cofinanced by the Région Alsace, the Centre National de la Recherche Scientifique, the Université Louis Pasteur, and the Association pour la Recherche sur le Cancer. We also thank the University of Utah, the Center for Biopolymers at Interfaces, and the National Institutes of Health (DC04336) for financial support of work on HA modification.

1. Decher, G. (1997) *Science* **277,** 1232–1237.
2. Decher, G., Hong, J. D. & Schmitt, J. (1992) *Thin Solid Films* **210,** 831–835.
3. Ladam, G., Schaaf, P., Cuisinier, F. G. J., Decher, G. & Voegel, J.-C. (2001) *Langmuir* **17,** 878–882.
4. Sukhorukov, G. B., Möhwald, H., Decher, G. & Lvov, Y. M. (1996) *Thin Solid Films* **284–285,** 220–223.
5. Chluba, J., Voegel, J. C., Decher, G., Erbacher, P., Schaaf, P. & Ogier, J. (2001) *Biomacromolecules* **2,** 800–805.
6. Elbert, D. L., Herbert, C. B. & Hubbell, J. A. (1999) *Langmuir* **15,** 5355–5362.
7. Picart, C., Lavalle, P., Hubert, P., Cuisinier, F. J. G., Decher, G., Schaaf, P. & Voegel, J. C. (2001) *Langmuir* **17,** 7414–7424.
8. Pardo-Yissar, V., Katz, E., Lioubashevski, O. & Willner, I. (2001) *Langmuir* **17,** 1110–1118.
9. Ruths, J., Essler, F., Decher, G. & Riegler, H. (2000) *Langmuir* **16,** 8871–8878.
10. Lavalle, P., Gergely, C., Cuisinier, F. J. G., Decher, G., Schaaf, P., Voegel, J. C. & Picart, C. (2002) *Macromolecules* **35,** 4458–4465.
11. McAloney, R. A., Sinyor, M., Dudnik, V. & Goh, M. C. (2001) *Langmuir* **17,** 6655–6663.
12. Decher, G. A., Lvov, Y. & Schmitt, J. (1994) *Thin Solid Films* **244,** 772–777.
13. Joly, S., Kane, R., Radzilowski, L., Wang, T., Wu, A., Cohen, R. E., Thomas, E. L. & Rubner, N. F. (2000) *Langmuir* **16,** 1354–1359.
14. Picart, C., Ladam, G., Senger, B., Voegel, J.-C., Schaaf, P., Cuisinier, F. J. G. & Gergely, C. (2001) *J. Chem. Phys.* **115,** 1086–1094.
15. Lapcik, L., Lapcik, L. L., De Smedt, S., Demeester, J. & Chabrechek, P. (1998) *Chem. Rev.* **98,** 2663–2684.
16. Laurent, T. C. (1998) *The Chemistry, Biology, and Medical Applications of Hyaluronan and Its Derivatives* (Cambridge Univ. Press, Cambridge, U.K.).
17. Gribbon, P., Heng, B. C. & Hardingham, T. E. (1999) *Biophys. J.* **77,** 2210–2216.
18. Maruyama, A., Ishihara, T., Kim, J.-S., Wan Kim, S. & Akaike, T. (1999) *Colloids Surf.* **153,** 439–443.
19. Mezo, G., Remenyi, J., Kajtar, J., Barna, K., Gaal, D. & Hudecz, F. (2000) *J. Control. Release* **63,** 81–95.
20. Cheng, Y. & Corn, R. M. (1999) *J. Phys. Chem.* **103,** 8726–8731.
21. Whitson, K. B., Lukan, A. M., Marlowe, R. L., Lee, S. A., Anthony, L. & Rupprecht, A. (1998) *Phys. Rev. E Stat. Phys. Plasmas Fluids Relat. Interdiscip. Top.* **58,** 2370–2377.
22. Fasman, G. D. (1976) *Handbook of Biochemistry and Molecular Biology* (CRC, Boca Raton, FL).
23. Pouyani, T. & Prestwich, G. D. (1994) *Bioconjugate Chem.* **5,** 339–347.
24. Luo, Y. & Prestwich, G. D. (1999) *Bioconjugate Chem.* **10,** 755–763.
25. Luo, Y., Kirker, K. R. & Prestwich, G. D. (2000) *J. Controlled Release* **69,** 169–184.
26. Prestwich, G. D. (2001) *Glycocoforum*, http://glycoforum.gr.jp/science/hyaluronan/HA18/HA18E.html.
27. Rodahl, M. & Kasemo, B. (1996) *Rev. Sci. Instrum.* **67,** 3238–3241.
28. Rodahl, M. & Kasemo, B. (1996) *Sensors Actuators B (Chemical)* **B37,** 111–116.
29. Hook, F., Rodahl, M., Brzezinski, P. & Kasemo, B. (1998) *J. Colloid Interface Sci.* **208,** 63–67.
30. Tiefenthaler, K. & Lukosz, W. (1989) *J. Opt. Soc. Am. B* **6,** 209–220.
31. Ramsden, J. J. (1997) *J. Mol. Recognit.* **10,** 109–120.
32. Nonogaki, T., Xu, S., Kugimiya, S., Sato, S., Niyata, I. & Yonese, N. (2000) *Langmuir* **16,** 4272–4278.
33. Fouissac, E., Milas, M., Rinaudo, M. & Borsali, R. (1992) *Macromolecules* **25,** 5613–5617.
34. Lee, S. A., Vansteenberg, M. L., Lavalle, N., Rupprecht, A. & Song, Z. (1994) *Biopolymers* **24,** 1543–1552.
35. Lee, W. I. & Schurr, J. M. (1974) *Biopolymers* **13,** 903–908.